RESEARCH ARTICLE

Cannabinoid receptor Type 1 densities reflect social organization in *Microtus*

Trenton C. Simmons[1] | Sara M. Freeman[1,2] | Nicholas S. Lackey[1] |
Brooke K. Dreyer[1] | Devanand S. Manoli[3] | Karen L. Bales[1]

[1]Department of Psychology, University of California, Davis, California

[2]Department of Biology, Utah State University, Logan, Utah

[3]Center for Integrative Neuroscience, University of California, San Francisco, California

Correspondence
Karen L. Bales, Department of Psychology, University of California, Davis, CA.
Email: klbales@ucdavis.edu

Abstract

Across many species, endocannabinoids play an important role in regulating social play, reward, and anxiety. These processes are mediated through at least two distinct cannabinoid receptors (CB), CB1 and CB2. CB1 expression is found in appreciable densities across regions of the brain that integrate memory with socio-spatial information; many of these regions have been directly linked to the neurobiology of pair bonding in monogamous species. Using receptor autoradiography, we provide the first distributional map of CB1 within the brains of closely related monogamous prairie voles and promiscuous meadow voles, and compare receptor densities across sexes and species in limbic regions. We observe CB1-specific signal using [3H] CP-55,940 and [3H] SR141716A, though the latter exhibited a lower signal to noise ratio. We confirmed the presence of CB2 in prairie vole spleen tissue using [3H] CP-55,940. However, we found no evidence of CB2 in the brain using either [3H] CP-55,940 or [3H] A-836,339. The overall distribution of putative CB1 in the brain was similar across vole species and followed the pattern of CB1 expression observed in other species—high intensity binding within the telencephalon, moderate binding within the diencephalon, and mild binding within the mesencephalon and metencephalon (aside from the cerebellar cortex). However, we found profound differences in CB1 densities across species, with prairie voles having higher CB1 binding in regions implicated in social attachment and spatial memory (e.g., periaqueductal gray, hippocampus). These findings suggest that CB1 densities, but not distribution, correlate with the social systems of vole species.

KEYWORDS

CB1, CB2, endocannabinoids, monogamy, pair bonding, social behavioral neural network

1 | INTRODUCTION

Ethologists have utilized a comparative approach to elucidate the selective pressures that drive the expression of sociality between species. Neuroscientists, on the other hand, have used similar approaches to highlight taxonomic differences in neural signaling systems. These methods have proven fruitful, revealing a critical role for nonapeptide hormones in regulating social behavior and providing a precedent for extending these approaches to novel signaling systems (Insel & Shapiro, 1992). In the present paper, we use a comparative approach modeled on Insel and Shapiro (1992) to examine differences in receptor maps across closely related species of voles that differ in their mating systems. Our study provides evidence that receptors of the endocannabinoid system may reflect the social organization of a species.

The endocannabinoid system is comprised of a network of receptors, ligands, and enzymes that were initially discovered through their

ability to mediate the effects of *Cannabis sativa* (Battista, Di Tommaso, Bari, & Maccarrone, 2012). The principal receptors for cannabis include the aptly named cannabinoid receptor Type 1, or CB1 (Matsuda, Lolait, Brownstein, Young, & Bonner, 1990) and Type 2, or CB2 (Munro, Thomas, & Abu-Shaar, 1993). The endocannabinoid system is widespread in mammals; CB1 has been labeled as one of the most prevalent metabotropic receptors in the brain (Pamplona & Takahashi, 2012), rivaling the expression levels of glutamate and GABA receptors. In the rodent brain, the highest densities of CB1 are found within the basal ganglia (Egertová & Elphick, 2000; Herkenham, Lynn, de Costa, & Richfield, 1991), hippocampus (HPC) (Herkenham et al., 1991; Jansen, Haycock, Ward, & Seybold, 1992), amygdala (AM; Ramikie et al., 2014; Yoshida et al., 2011) and cerebellum (Egertová & Elphick, 2000; Herkenham et al., 1991; Matsuda, Bonner, & Lolait, 1993), suggesting an important role for the endocannabinoid system in modulating complex behaviors.

Historically, it was thought that CB1 was only expressed on neuronal tissues while CB2 was specific to immune cells in the periphery (Hu & Mackie, 2015). Recent evidence provides a more nuanced yet controversial picture of cannabinoid receptor expression. For example, studies have confirmed the presence of CB1 in nonneuronal tissue, such as myelinating Schwann cells (Freundt-Revilla, Kegler, Baumgärtner, & Tipold, 2017), while others suggest that CB2 may be expressed in the brain stem (Van Sickle et al., 2005). The presence of CB2 in the central nervous system (CNS) has been demonstrated primarily with immunohistochemical approaches and concerns have risen regarding an apparent lack of specific antibodies against CB2 protein (Atwood & Mackie, 2010). One study addressed the controversy using a novel reporter mouse line and found no evidence of CB2 in the CNS of healthy mice; in addition, CB2 was detected in spleen samples of healthy reporter mice but not in CB2 knockout mice (Lopez et al., 2018). However, CB2 expression was found in the CNS of mice with familial Alzheimer's disease mutations, particularly in areas of intense inflammation and amyloid deposition. These results suggest that CB2 may be expressed within the brain under pathological but not neurotypical conditions.

A preponderance of the literature suggests that the neural circuitry of disparate social behaviors overlaps greatly. This complex neural framework for sociality has been labeled the "social behavior neural network" (SBNN) and consists of neural regions that fulfill specific criteria (Albers, 2015; Newman, 1999); these regions are reciprocally connected, express receptors for gonadal hormones, and have been critically linked to regulation of multiple social behaviors. The original model of the SBNN included regions like the extended AM, lateral septum (LS), periaqueductal gray (PAG), medial preoptic area (MPA), ventromedial hypothalamus (VMH), and anterior hypothalamus (AH). Collectively, these regions regulate a wide range of social behaviors, including communication, reproduction, parenting, individual recognition, and memory (Newman, 1999). Thus, signaling systems that modulate social behavior should be expressed within these regions. Previous studies suggest that CB1 are indeed found in each of these regions in rats, humans, rhesus monkeys, dogs, and guinea pigs (Herkenham et al., 1990).

In addition to expression within the SBNN, several other observations regarding the cannabinoid system implicate its function in the regulation of social behavior. These include species differences, sex differences, individual variation, modulation by gonadal hormones and modulation by social factors (Albers, 2015). Interestingly, the regional distribution of CB1 is largely conserved across different mammalian species, suggesting a more fundamental role for endocannabinoid signaling in the regulation of neuronal activity (Herkenham et al., 1990). However, there are subtle differences in density across species that are in part explained by species-typical behavior. For example, humans had greater binding density in the basolateral amygdala (BLA) than other species (Herkenham et al., 1990). Endocannabinoids are also implicated in the regulation of social behavior by the oxytocin system. Oxytocin has been very widely studied as a neurohormone underlying social behavior in mammals (Carter, 1998; Grinevich & Neumann, 2020). Recent evidence suggests that oxytocin mobilizes anandamide and then facilitates social behavior through the CB1 receptor (Wei et al., 2015). As oxytocin receptor also varies by social structure in voles (Insel & Shapiro, 1992), one might hypothesize a similar variation in distribution of CB1.

There are also sex differences in CB1 expression; male rats had higher CB1 densities in the prefrontal cortex (PFC) and AM than both cycling and ovariectomized females (Castelli et al., 2014). These results were likely estradiol-dependent, since the sex differences were lost when ovariectomized females had estradiol replaced. Similarly, castrated male rats had decreased CB1 densities that were restored to control values after testosterone replacement (Busch, Sterin-Borda, & Borda, 2006).

Finally, there is also evidence that the endocannabinoid system is modulated by social factors on an individual level. In starlings, males who sang to females, had nesting sites, and displaced other males had increased CB1 densities in the LS and the robust nucleus of the arcopallium (DeVries, Cordes, Rodriguez, Stevenson, & Riters, 2016), an analog of the AM in birds. This study also showed that CB1 expression within the LS was positively correlated with the frequency of measured agonistic behaviors while expression in the robust nucleus of the arcopallium was negatively correlated with singing behavior. As shown, CB1 demonstrate all the properties that would be expected from a signaling system that underlies sociality.

The many species of vole belonging to the genus *Microtus* exhibit similar nonsocial behaviors (Tamarin, 1985). For example, both prairie voles (*Microtus ochrogaster*) and meadow voles (*Microtus pennsylvanicus*) can dig and subsequently create extensive networks of aboveground runways and underground tunnels that interconnect feeding areas, waterways, and nested shelters. Similarly, both species engage in swimming behavior and exclusively use grasses for nests. Locomotor behaviors are also highly conserved in *Microtus*; both prairie and meadow voles exhibit thigmotaxis, rearing, grooming, and freezing behavior.

While the nonsocial behaviors of *Microtus* are highly conserved, the organization of social behaviors for each species is widely variable (Tamarin, 1985). In both natural and laboratory settings, prairie voles form monogamous attachments that persist across multiple breeding

seasons (and also fail to demonstrate Coolidge effect) while meadow voles have a promiscuous mating system (Getz, Carter, & Gavish, 1981; Gruder-Adams & Getz, 1985). Prairie voles are biparental, and older pups frequently remain in the nest to contribute care to pups from succeeding litters (Carter, DeVries, & Getz, 1995; Roberts, Miller, Taymans, & Carter, 1998; Roberts, Williams, Wang, & Carter, 1998). Conversely, meadow voles are socially organized into territorial maternal-young groups during the breeding season and form communal mixed-sex groups during the winter (Boonstra, Xia, & Pavone, 1993; Gruder-Adams & Getz, 1985).

Comparative approaches using the *Microtus* model have historically offered a unique opportunity to explore the neurological underpinnings of sociality (Carter et al., 1995; Shapiro & Insel, 1992). Specifically, Insel and Shapiro (1992) pioneered this approach with monogamous prairie voles and promiscuous montane voles (*Microtus montanus*) to demonstrate that the neural distribution of oxytocin receptors reflected differences in the social structure between species. In prairie voles, oxytocin receptor density was highest in several limbic regions, including the prelimbic cortex, bed nucleus of the stria terminalis (BST), nucleus accumbens (NAc), medial thalamus, and the lateral AM; each of these regions had very little binding in montane voles. On the other hand, oxytocin receptor density in montane voles was strongest in the LS, VMH, and cortical nucleus of the AM. Insel and Shapiro recapitulated their findings using two additional species of *Microtus*, the monogamous pine vole (*Microtus pinetorum*) and the promiscuous meadow vole, while demonstrating a lack of similar species differences in other neurotransmitter systems (benzodiazepines, mu opioids) which also play a role in mediating social behavior. Taken together, these findings suggest a comparative approach using species of *Microtus* can help target key neural substrates that contribute to the SBNN.

Our objective with the present study was fourfold: (a) validate receptor autoradiography techniques for cannabinoid receptors in voles, (b) provide the first map of cannabinoid receptors in both the prairie vole and meadow vole brains, (c) conduct intersex comparisons within each species, and (d) conduct interspecies comparisons within each sex (pending sex differences). Since CB1 distribution is highly conserved across species, we expected to find similar distributions of CB1 in brain regions across species, including the cerebellum, basal ganglia, cortex, and limbic regions. For sex comparisons, we predicted that males would have higher CB1 densities in the PFC and AM. For species comparisons, we expected to find density differences across species throughout the nodes of the SBNN. Finally, since we only examined patterns of binding in healthy adult voles, we expected to find no evidence of CB2 expression in the brain.

2 | MATERIALS AND METHODS

2.1 | Subjects

Our study utilized 57 prairie voles from the breeding colony located in the Psychology department of the University of California, Davis,

CA. They were maintained on a 14:10 hr light cycle at approximately 21°C and had access to food (Purina High Fiber Rabbit Chow, PMI Nutrition International, Brentwood, MO) and water ad libitum. The animals were housed with their parents in large polycarbonate cages (44 × 22 × 16 cm) until weaning at postnatal day (P) 20. Subjects were then separated from their parents, given ear-clip markings for identification, and placed with a same-sex sibling in smaller cages (27 × 16 × 13 cm) through adulthood.

For interspecies comparisons in Experiment 4, we also acquired 21 meadow vole brains from the breeding colony located at the University of California, San Francisco. The meadow voles were maintained on a 14:10 hr light cycle at 21°C and had constant access to water and Mouse Diet 5015. Subjects also received Laboratory Rabbit Diet HF, apples, yams, and chard twice a week during cage changes. All subjects were housed with their parents in Ancare R20 Rat Cages (48 × 20 × 27 cm) with nesting huts until weaning approximately on P 20. Subjects were weaned into Innovive Conventional Rat Cages (37.3 × 23.4 × 14.0 cm) with a density of six animals per cage and given ear tags for identification until adulthood.

All animals were sacrificed as adults and brains were collected, flash-frozen on dry ice, and stored at −80°C; the average age was comparable across species (prairie voles: $M = 77$ days, $SD = 7.55$ days; meadow voles: age: $M = 74$ days; 8.83 days). Animal care and euthanasia procedures followed National Institutes of Health guidelines and were approved by the Animal Care and Use Committees at the University of California, Davis and University of California, San Francisco. Prairie voles were used throughout all four experiments while meadow voles were only used in Experiment 4.

2.2 | Autoradiography

We used the nonspecific CB1-CB2 radioligand [3H] CP-55,940 (PerkinElmer, Boston, MA), the CB1-selective radioligand [3H] SR141716A (PerkinElmer), and the CB2-selective radioligand [3H] A-836,339 (Metis Labs, Ronkonkoma, NY) to produce quantifiable autoradiographic signals. These radioligands were coincubated with or without one of three unlabeled ligands to produce competitor conditions in order to assess nonspecific binding: the CB1 ligand AM251 (Tocris, Minneapolis, MN) and the CB2 ligands HU308 (Tocris) or SR144528 (Tocris) (Table 1).

Brain tissue sectioned at 20 μm were obtained from the anterior pole of the forebrain to the cerebellum and mounted onto Super-frost slides for storage at −80°C. Our receptor autoradiography procedures were completed in a series of four experiments with varying radioligands and competitors. On the day of receptor autoradiography, we thawed the tissue to room temperature and immersed it in 0.1% paraformaldehyde for 2 min. Slides were rinsed for 2 × 10 min in 50 mM Tris–HCl buffer (pH 7.4) and then incubated with the radioligand with or without an unlabeled competitor (see Table 1) for 90 min in a solution of 50 mM Tris–HCl (pH 7.4) with 0.2% MgCl₂, and 0.1% bovine serum albumin. Following the incubation, slides were washed in 50 mM Tris–HCl buffer (pH 5.4) with 5% MgCl2 for 2 × 10 min at

TABLE 1 Competitive binding assay conditions

	Condition		
	Radioligand	**Competitor?**	**Purpose**
Experiment 1 (n = 14)			*Radioligand validation in brain tissue*
Set A	1 nM [3H] CP-55,940	—	Visualize CB1/CB2 binding
Set B	1 nM [3H] CP-55,940	25 nM HU308	Block CB2 binding
Set C	1 nM [3H] CP-55,940	10 nM AM251	Block CB1 binding
Experiment 2 (n = 21)			*Radioligand validation in brain tissue*
Set A	2 nM [3H] SR141716A	—	Visualize CB1 binding
Set B	2 nM [3H] SR141716A	10 nM AM251	Determine off-target binding
Set C	1 nM [3H] A-836,339	—	Visualize CB2 binding
Set D	1 nM [3H] A-836,339	1 nM SR144528	Determine off-target binding
Experiment 3 (n = 8[a])			*Radioligand validation in spleen tissue*
Set A	2 nM [3H] SR141716A	—	Visualize CB1 binding
Set B	2 nM [3H] SR141716A	1 μM AM251	Determine off-target binding
Set C	1 nM [3H] A-836,339	—	Visualize CB2 binding
Set D	1 nM [3H] A-836,339	1 nM SR144528	Determine off-target binding
Set E	1 nM [3H] CP-55,940	—	Visualize CB1/CB2 binding
Set F	1 nM [3H] CP-55,940	1 μM HU308	Block CB2 binding
Set G	1 nM [3H] CP-55,940	1 μM AM251	Block CB1 binding
Experiment 4 (n = 43)			*CB1 mapping study in brain tissue*
Set A	1 nM [3H] CP-55,940	—	Visualize CB1[b] binding

[a]Spleens obtained from subjects in Experiment 2.
[b]Experiment 1 confirms 1 nM [3H] CP-55,940 prioritizes CB1.

4°C, and 30 min at room temperature before a final dip in cold dH20. Once the slides were dry, they were opposed to Kodak Carestream BioMax MR film (Kodak, Rochester, NY) with a set of 14 ^{3}H microscale standards (American Radiolabeled Chemicals, Inc., St. Louis, MO) for 6 weeks and developed for subsequent quantification. The concentrations of the ligands used in our assays are listed in Table 1 and were chosen to reflect their individual binding affinities for either CB1 or CB2 in rodents (Pertwee, 2010). In a multiple alignment between prairie voles, mice, and rats, based on CB1 amino acid sequences and performed in NCBI's protein BLAST tool, there are only seven amino acid positions that differ between prairie voles and the other two rodents. The percent identical between prairie voles and rats are 98.73%, and prairie vole and mouse CB1 are 98.52% identical. Unfortunately, the meadow vole sequence was not available; however, they are a closely related species of the same genus as prairie voles (Tamarin, 1985).

2.3 | Imaging and quantification

Our autoradiographs were quantified using the MCID Digital Densitometry Core System (Interfocus Imaging, Cambridge, UK). Using the microscale standards, we created a calibration curve that extrapolated all optical binding density measurements into standardized nCi/mg values. Areas with nonbackground amounts of signal were then

quantified by taking the average of three representative sections, and these values were normalized by subtracting off the average nonspecific binding, taken from an average of three measures of background. The background measure of nonspecific binding was made in a brain area with no specific radioligand binding signal (corpus callosum) and was performed identically for both species. As evidence for laterality in endocannabinoid signaling is sparse, measurements were only taken from the anatomical left side of the brain.

2.4 | Statistical analyses

All comparisons were planned a priori and varied from experiment to experiment. In the radioligand validation experiments (1–3), conditions with competitors were compared directly to conditions without (e.g., [3H] SR141716A vs. [3H] SR141716A + AM251). In Experiment 4, we began by comparing the binding of the radioligand alone in each region of interest across sexes within species to test for sex differences. No sex differences were found for any region we measured, so we collapsed across sex for subsequent comparisons across species.

We used R version 3.5.3 (R Core Team, 2019) to conduct one-way analyses of variance (ANOVAs) on each outcome measure. For the validation experiments (1–3), binding density was analyzed with condition as the fixed effect. Post hoc analyses were performed on any models with a significant effect for condition and only

comparisons to control were made, warranting the use of Dunnett's test to help control for Type I errors. For Experiment 4, ANOVA were initially conducted on each region within species with sex as the fixed effect. When sex differences were absent, data from each sex were binned together and subsequent ANOVA were conducted with species as the fixed effect. Post hoc analyses were performed on any models with a significant effect for species and p values were adjusted for multiple comparisons using the familywise detection rate. All models regardless of experiment met the assumptions for ANOVA testing, which were confirmed for each analysis using the Shapiro–Wilk and Levene's tests. Significance was determined at α = .05. ANOVA modeling and post hoc comparisons were accomplished using the effsize package (Torchiano, 2018).
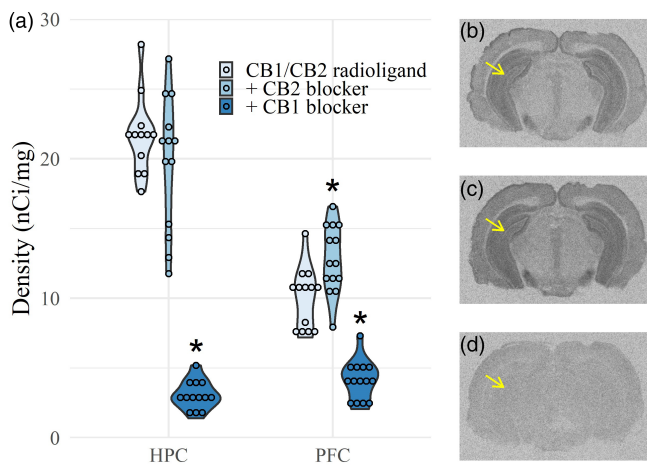

FIGURE 1 Validation of [3H] CP-55,940 for autoradiography in prairie vole brains. Three adjacent sections of brain tissue were incubated with [3H] CP-55,940 with or without an unlabeled receptor competitor. Coincubation of the radioligand with the CB2 blocker (HU308) had no discernible impact on binding in the hippocampus (HPC) but increased binding in the prefrontal cortex (PFC) relative to control. Coincubation of the radioligand with the CB1 blocker (AM251) significantly decreased signal in both regions. Representative autoradiographs depict each condition at the level of the HPC. *p < .05 [Color figure can be viewed at wileyonlinelibrary.com]

3 | RESULTS

3.1 | Experiment 1: [3H] CP-55,940 validation in brain tissue

For validation purposes, we selected two regions with appreciable amount of signal, the HPC and PFC, and quantified them for comparisons across competitor conditions. We found a significant effect of assay condition on the HPC ($F(3,35)$ = 123.9, p < .0001]; [3H] CP-55,940 binding in the alone condition was greater than binding with AM251 ($t(35)$ = 14.154, p < .0001) (Figure 1). Assay condition also impacted the PFC ($F(2,39)$ = 40.6, p < .0001), in which binding from the nonselective CB1-CB2 radioligand [3H] CP-55,940 alone was lesser than binding when coincubated with the unlabeled CB2 ligand HU308 ($t(39)$ = −3.586, p = .002) and greater than binding when coincubated with the unlabeled CB1 ligand AM251 ($t(39)$ = 5.366, p < .0001) (Figure 1). The observation that coincubation with the CB1-specific ligand, AM251, effectively removed all appreciable radioligand binding from the HPC and PFC supports the conclusion that CB1 is the only cannabinoid receptor expressed in these regions. Also, coincubation with the CB2-specific ligand, HU308, had either no effect or increased radioligand binding.

3.2 | Experiment 2: [3H] SR141716A and [3H] A-836,339 validation in brain tissue

Like Experiment 1, we quantified the PFC and HPC for comparisons across competitor conditions. We found no effect of competitor on CB1-selective radioligand [3H] SR141716A binding in the PFC ($F(1,54)$ = 2.844, p = .0975) and a significant effect in the HPC ($F(1,54)$ = 29.66, p < .0001). Specifically, coincubation with CB1 ligand AM251 decreased [3H] SR141716A binding in the HPC ($t(54)$ = 5.446, p < .0001) (Figure 2). These data suggest that the signal to noise ratio might be smaller with [3H] SR141716A than with
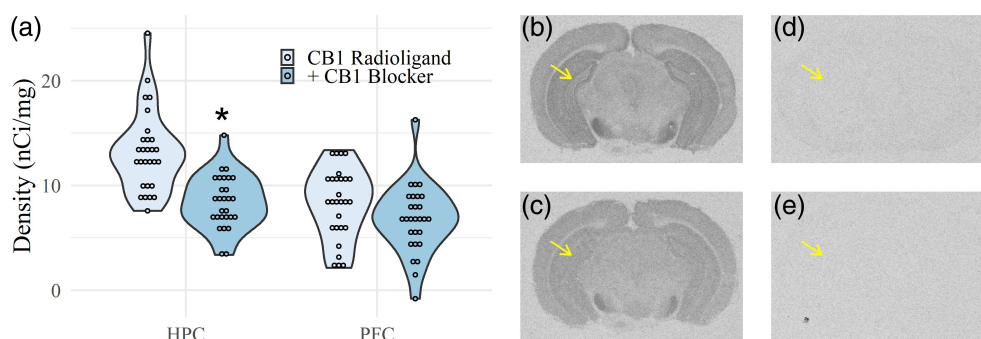

FIGURE 2 Validation of [3H] SR141716A and [3H] A-836,339 for autoradiography in prairie vole brains. Four adjacent sections of brain tissue were incubated with radioligand that was specific for CB1 ([3H] SR141716A) or CB2 ([3H] A-836,339) with complementary blockers for the same receptor. Coincubation of [3H] SR141716A with AM251 decreased signal in the hippocampus (HPC) but not in the prefrontal cortex (PFC). Neither the [3H] A-836,339 condition with or without the competitor (HU308) produced quantifiable levels of signal. Representative autoradiographs depict each condition at the level of the HPC. *p < .05 [Color figure can be viewed at wileyonlinelibrary.com]

[3H] CP-55,940 given the difference in results for the PFC between the two experiments.

To pursue our CB2 findings from Experiment 1, we conducted an additional assay using the CB2-specific radioligand [3H] A-836,339. We found no evidence of appreciable binding across any section of brain tissue that was greater than background (Figure 2). These results combined with those from Experiment 1 suggest difficulty in using radioligands to visualize CB2 in brain tissue.

3.3 | Experiment 3: Radioligand validation in spleen tissue

The presence of CB2 binding in the brain has been controversial for decades (Atwood & Mackie, 2010). Given our inability to detect CB2 in the brain, we decided to assay spleen tissue as a positive control since spleens do contain CB2 in other species (Lopez et al., 2018). We found no effect of condition on [3H] SR141716A binding ($F_{(1,14)}$ = 3.945, p = .0669) and were not able to detect any appreciable amount of [3H] A-836,339 binding in prairie vole spleens (Figure 3). However, we did find a significant effect of condition on [3H] CP-55,940 binding in spleen
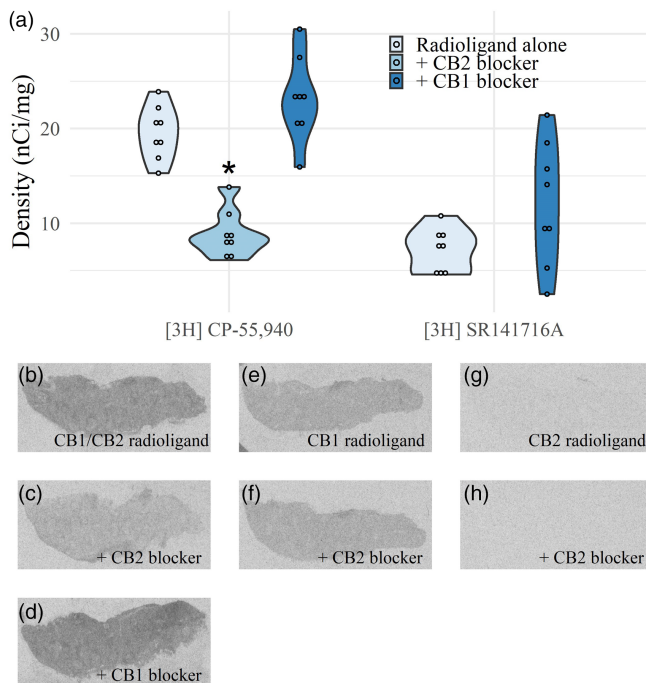
FIGURE 3 Validation of [3H] CP-55,940, [3H] SR141716A and [3H] A-836,339 for autoradiography in prairie vole spleens. Seven adjacent sections of spleen tissue were incubated with radioligand that was coincubated with or without unlabeled blockers. [3H] CP-55,940 signal was decreased when coincubated with HU308 (CB2 blocker) but not with AM251 (CB1 blocker). [3H] SR141716A signal was not significantly impacted by AM251 competition. We found no evidence of [3H] A-836,339 signal in spleen assay with or without a CB2 competitor (SR144528). *p < .05 [Color figure can be viewed at wileyonlinelibrary.com]

tissue ($F_{(2,21)}$ = 38.83, p < .0001). Specifically, coincubation with HU308 decreased [3H] CP-55,940 binding ($t_{(21)}$ = 6.357, p < .0001) (Figure 3). These results confirm that autoradiographic techniques can be used with [3H] CP-55,940, with a CB2 specific competitor, to visualize CB2 in vole species. These results also suggest that either CB2 is not found in appreciable amounts in the healthy prairie vole brain, or that the purportedly selective ligand [3H]A-836,339 does not work.

3.4 | Experiment 4: Mapping cannabinoid receptors in *Microtus*

3.4.1 | Distribution of cannabinoid receptors in *Microtus*

Our validation experiments suggest that autoradiography with 1 nM [3H] CP-55,940 alone sufficiently and selectively binds CB1 in prairie vole brain tissue. We did not perform the CB2 study with meadow vole spleen, and thus cannot conclusively eliminate the possibility that meadow voles express CB2 in the brain (despite the high homology across mammalian species). This is a caveat to our purported CB1 receptor distributions below, in that it is possible that for meadow voles we are measuring a mix of CB1 and CB2 receptor. We selected 1 nM [3H] CP-55,940 for use in our mapping study (Figure 4).

CB1 was found throughout most of the forebrain (Table 2). Moderate binding was detected in the main and accessory olfactory bulbs (MOB and AOB, respectively) and anterior olfactory nucleus (AON). Of these structures, the densest binding was in the AON.

CB1 density was widespread throughout the cortex, including areas like the orbitofrontal cortex (ORB), PFC, anterior cingulate cortex (ACC), primary motor cortex (M1), primary somatosensory cortex (S1), piriform (PIR), posterior cingulate cortex (PCC), primary visual cortex (V1), primary auditory cortex (A1), and entorhinal cortex (ENT). Each of these regions contained similar levels of CB1 with the highest binding in the ORB.

Moderate CB1 binding was found in the NAc and caudate-putamen (CP), while binding in the ventral pallidum (VP) was lower. The globus pallidus also contained CB1, with denser binding in the external globus pallidus (GPe) than in the internal (GPi). The LS and BST displayed moderate binding.

CB1 binding was evenly distributed throughout the nuclei of the AM. We specifically detected moderate binding in the BLA, basomedial amygdala (BMA), central amygdala (CEA), and medial amygdala (MEA). However, the densest binding within the forebrain was found in the HPC. Moderately high levels of CB1 were measured in subfields CA1, CA2, and CA3 along with the subiculum (SUB) and dentate gyrus (DG).

The diencephalon also contained mild to moderate CB1 binding. Specifically, CB1 was detected throughout hypothalamic structures, including the MPA, AH, lateral nucleus (LH), and mammillary bodies (MBO). Binding within the LH was the least dense of the hypothalamic structures. Within the thalamus, CB1 binding was found in the

laterodorsal nucleus (LDTh), mediodorsal nucleus (MDTh), and ventroposterior nucleus (VPTh). The VPTh contained the mildest amount of CB1 binding.

Within the midbrain, CB1 were sparse in the reticular formation (MRF). Moderate CB1 densities were detected in the ventral tegmental area (VTA), PAG, superior colliculus (SC), inferior colliculus (IC), and the interpeduncular nucleus (IPN). High CB1 binding was found in the substantia nigra (SN) with levels greater than the HPC.

Our sectioning ended with the cerebellum and did not include an appreciable amount of pons and medulla tissue. However, the most intense CB1 binding detected throughout the entirety of the brain was in the molecular layer of the cerebellar cortex (CBX). We were unable to detect CB1 in the granular layer. We also detected mild to moderate levels of bindings within the pontine gray (PG).

3.4.2 | Sex and species comparisons

We compared putative CB1 densities in all reported regions across sexes and within species. We found no evidence for sex differences in either species for any of the 45 regions analyzed (Tables 3 and 4). Consequently, we collapsed across sex for interspecies comparisons. Furthermore, we only analyzed species differences in limbic regions since the purpose of this study was to determine whether the social organization of a species is reflected in the density of CB1. We found a statistically significant effect of species on many limbic regions, including the AH, BST, CA1, CA2, CA3, DG, LDTh, LS, MBO, MDTh, MPN, MRN, PAG, SUB, and VPTh (Table 5). Following adjustments for multiple comparisons, significant effects remained for CA2, CA3, DG, LDTh, MBO, MDTh, PAG, and VPTh (Figure 5). Prairie voles had higher CB1 densities than meadow voles in each of these regions.

4 | DISCUSSION

The present study demonstrates the utility of autoradiographic techniques to selectively visualize both CB1 densities in vole tissue, and the differential density of CB1 binding in mammals that demonstrate promiscuous versus monogamous mating strategies and distinct levels of affiliative behaviors between conspecifics. We found no evidence for CB2 in the prairie vole brain but confirmed the ability of our methods to detect the receptor in spleen tissue. Our techniques also reveal an almost ubiquitous expression of CB1 across the vole brain that matches the distribution and density trends of other species.
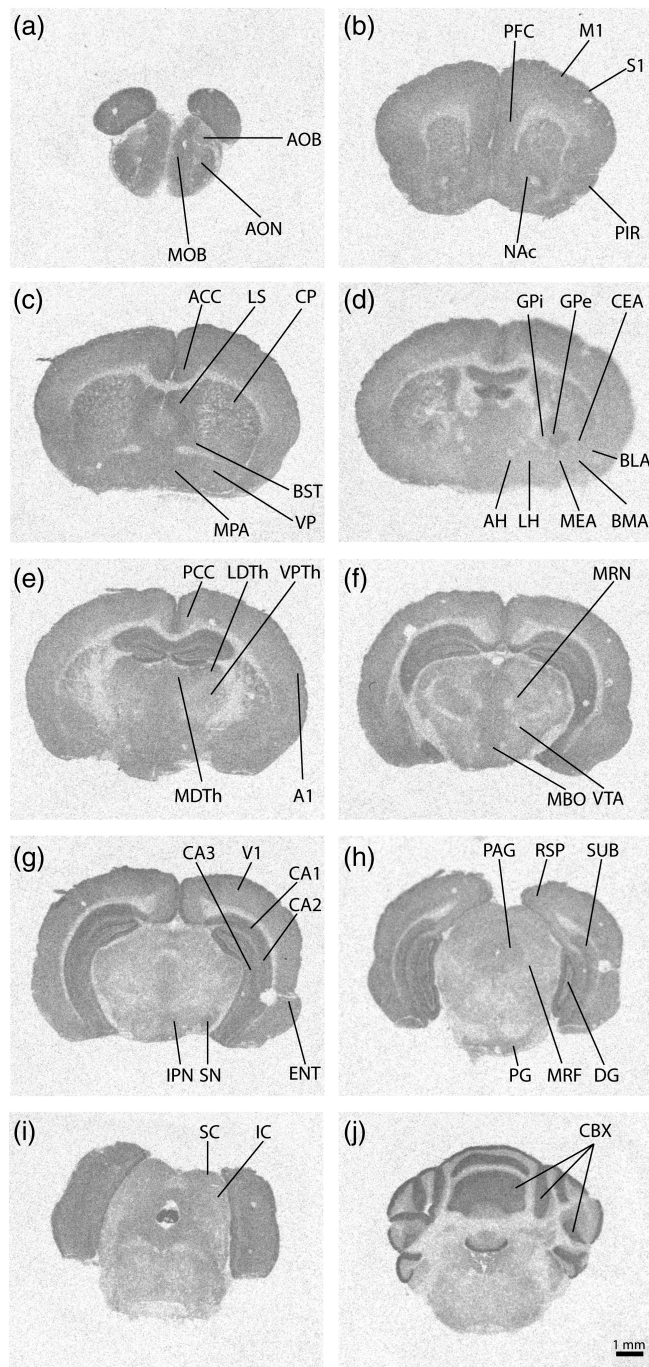

FIGURE 4 Representative autoradiograms of CB1 receptors, mapped with [3H] CP-55,940, throughout prairie vole brain. A1, primary auditory cortex; ACC, anterior cingulate cortex; AH, anterior hypothalamus; AOB, accessory olfactory bulb; AON, anterior olfactory nucleus; BLA, basolateral amygdala; BMA, basomedial amygdala; BST, bed nucleus of the stria terminalis; CBX, cerebellar cortex; CEA, central amygdala; CP, caudate-putamen; DG, dentate gyrus; ENT, entorhinal cortex; GPe, globus pallidus external; GPi, globus pallidus internal; IC, inferior colliculus; IPN, interpeduncular nucleus; LDTh, laterodorsal thalamus; LH, lateral hypothalamus; LS, lateral septum; MBO, mammillary bodies; MDTh, mediodorsal thalamus; MEA, medial amygdala; M1, primary motor area; MOB, main olfactory bulb; MPA, medial preoptic area; MRF, reticular formation; MRN, median raphe nucleus; NAc, nucleus accumbens; ORB, orbitofrontal cortex; PAG, periaqueductal gray; PCC, posterior cingulate cortex; PFC, prefrontal cortex; PG, pontine gray; PIR, piriform cortex; RSP, retrosplenial cortex; S1, primary somatosensory cortex; SC, superior colliculus; SN, substantia nigra; SUB, subiculum; V1, primary visual cortex; VP, ventral pallidum; VPTh, ventroposterior thalamus; VTA, ventral tegmental area

TABLE 2 Relative binding density across region

Telencephalon	Prairie	Meadow	Diencephalon	Prairie	Meadow
Olfactory bulb			*Thalamus*		
MOB	+++	+++	LDTh	++	++
AOB	++	++	VPTh	+	+
AON	+++	+++	MDTh	++	++
Cortex			*Hypothalamus*		
PFC	+++	+++	AH	++	++
ACC	+++	+++	LH	+	+
PCC	+++	++	MPN	++	++
M1	+++	+++	MBO	++	++
S1	++	+++			
V1	++	+++	**Mesencephalon**	**Prairie**	**Meadow**
A1	++	++	IC	++	++
PIR	++	+++	IPN	++	++
ENT	+++	++	MRF	+	+
ORB	+++	++++	PAG	++	++
Basal nuclei			SC	++	++
CP	++	++	SN	++++	++++
GPe	++	++	VTA	++	++
GPi	+	+			
VP	++	++	**Metencephalon**	**Prairie**	**Meadow**
Hippocampus			CBX	++++	++++
CA1	++++	++++	PG	++	+
CA2	++++	++++			
CA3	+++	+++			
SUB	+++	+++			
DG	++++	+++			
Amygdala					
CEA	++	++			
MEA	++	++			
BMA	++	++			
BLA	++	++			
Other					
NAc	++	+++			
LS	+++	+++			
BST	++	++			

Note: Average densities were taken for each area and then the entire distribution for each species was divided into quartile sections. The number of plus signs thus represents the quartile bin containing the average binding density for each area. Specifically, +, first quartile; ++, second quartile; +++, third quartile; ++++, fourth quartile.

Abbreviations: AM, amygdala; BMA, basomedial amygdala; BST, bed nucleus of the stria terminalis; CBX, cerebellar cortex; DG, dentate gyrus; GPe, globus pallidus external; GPi, globus pallidus internal; HPC, hippocampus; LDTh, laterodorsal thalamus; MBO, mammillary bodies; MDTh, mediodorsal thalamus; MEA, medial amygdala; NAc, nucleus accumbens; ORB, orbitofrontal cortex; PAG, periaqueductal gray; VPTh, ventroposterior thalamus.

Additionally, we did not detect any evidence of sex differences across any of the regions we measured in either species. However, our comparative approach found that prairie voles generally express more putative CB1 throughout many regions of brain than meadow voles, especially across the nodes of the SBNN.

Our validation experiments utilized several commercial cannabinoid receptor radioligands with variable binding affinities for both cannabinoid receptors. [3H] CP-55,940, for example, is an indiscriminate cannabinoid receptor radioligand that binds to both CB1 and CB2 with comparable binding affinities (Pertwee, 2000). Using

TABLE 3 Binding density by sex in prairie voles

Region	Females M (SEM)	Males M (SEM)	One-way ANOVA test statistics			Post hoc test statistics	
			F	df	p	d	p-Adjusted
ACA	17.2 (1.3)	16.4 (1.0)	0.224	2, 18	.641	0.212 [−0.730, 1.154]	.890
ACB	14.3 (1.6)	13.9 (1.7)	0.030	2, 20	.863	0.074 [−0.815, 0.964]	.900
AH	11.2 (1.2)	13.3 (1.3)	1.525	2, 20	.231	0.527 [−1.431, 0.378]	.890
BLA	13.3 (1.3)	12.7 (1.1)	0.171	2, 19	.684	0.181 [−0.736, 1.097]	.890
BMA	10.4 (0.8)	10.8 (0.9)	0.098	2, 19	.757	0.137 [−1.053, 0.779]	.890
BST	11.9 (1.0)	11.4 (1.0)	0.087	2, 20	.771	0.126 [−0.765, 1.016]	.890
CA1	24.4 (0.9)	23.3 (2.5)	0.181	2, 20	.675	0.181 [−0.710, 1.072]	.890
CA2	24.3 (1.1)	24.2 (2.0)	0.001	2, 20	.970	0.016 [−0.873, 0.906]	.970
CA3	23.4 (1.0)	21.7 (2.2)	0.479	2, 20	.497	0.295 [−0.599, 1.189]	.890
CEA	11.2 (1.1)	10.7 (0.9)	0.131	2, 19	.721	0.158 [−0.758, 1.074]	.890
CP	12.5 (1.1)	11.3 (1.4)	0.492	2, 20	.491	0.299 [−0.595, 1.193]	.890
DG	22.6 (1.6)	24.3 (1.2)	0.704	2, 20	.411	0.358 [−1.254, 0.539]	.890
GPe	10.9 (1.5)	11.5 (1.1)	0.109	2, 20	.744	0.141 [−1.032, 0.750]	.890
GPi	6.7 (0.7)	6.0 (0.8)	0.468	2, 19	.502	0.299 [−0.621, 1.218]	.890
LDTh	10.2 (1.1)	11.1 (1.0)	0.403	2, 19	.533	0.277 [−1.196, 0.641]	.890
LH	5.8 (1.0)	6.9 (0.8)	0.897	2, 20	.355	0.404 [−1.302, 0.495]	.890
LS	16.6 (1.6)	16.0 (1.3)	0.093	2, 20	.763	0.130 [−0.760, 1.021]	.890
MBO	11.7 (1.3)	10.4 (1.2)	0.499	2, 20	.488	0.301 [−0.593, 1.196]	.890
MDTh	11.0 (1.0)	11.9 (1.0)	0.404	2, 19	.532	0.278 [−1.197, 0.641]	.890
MEA	9.0 (0.8)	9.7 (0.8)	0.274	2, 19	.607	0.229 [−1.146, 0.689]	.890
MPN	12.0 (1.2)	12.3 (0.9)	0.053	2, 20	.820	0.098 [−0.988, 0.792]	.900
MRN	5.0 (0.9)	5.7 (0.5)	0.379	2, 20	.545	0.263 [−1.156, 0.631]	.890
PAG	12.7 (1.1)	14.0 (0.9)	0.761	2, 20	.393	0.372 [−1.269, 0.525]	.890
PFC	16.8 (1.4)	15.9 (1.4)	0.189	2, 20	.668	0.185 [−0.706, 1.077]	.890
RSP	14.3 (1.6)	16.3 (1.1)	0.947	2, 19	.343	0.425 [−1.350, 0.499]	.890
SN	28.8 (1.9)	29.4 (2.9)	0.028	2, 20	.870	0.071 [−0.960, 0.819]	.900
SUB	20.1 (1.7)	21.2 (1.2)	0.276	2, 20	.605	0.224 [−1.116, 0.668]	.890
VPTh	5.9 (0.8)	6.9 (0.9)	0.553	2, 19	.466	0.325 [−1.245, 0.596]	.890
VP	9.3 (1.2)	10.8 (1.3)	0.687	2, 20	.417	0.353 [−1.250, 0.543]	.890
VTA	8.9 (0.8)	8.5 (1.1)	0.114	2, 20	.739	0.144 [−0.746, 1.035]	.890

Abbreviations: AH, anterior hypothalamus; BLA, basolateral amygdala; BMA, basomedial amygdala; BST, bed nucleus of the stria terminalis; CEA, central amygdala; CP, caudate-putamen; DG, dentate gyrus; GPe, globus pallidus external; GPi, globus pallidum internal; LDTh, laterodorsal thalamus; LH, lateral hypothalamus; LS, lateral septum; MBO, mammillary bodies; MDTh, mediodorsal thalamus; MEA, medial amygdala; MOB, main olfactory bulb; MPA, medial preoptic area; MRF, reticular formation; MRN, median raphe nucleus; NAc, nucleus accumbens; PAG, periaqueductal gray; PFC, prefrontal cortex; PG, pontine gray; RSP, retrosplenial cortex; SC, superior colliculus; SN, substantia nigra; SUB, subiculum; VP, ventral pallidum; VPTh, ventroposterior thalamus; VTA, ventral tegmental area.

competitive binding assays, we were able to use this radioligand and unlabeled competitors to selectively visualize CB1 in the brain and CB2 in the prairie vole spleen. However, we were unable to detect signal in any of the tissues tested using the CB2-specific radioligand [3H] A-836,339. To our knowledge, [3H] A-836,339 is also the only commercially available radioligand for CB2, but it has not been used for autoradiography in the past. In addition, the CB1-specific radioligand [3H] SR141716A decreased the signal to noise ratio when compared to [3H] CP-55,940, resulting in a failure to detect significant CB1 signal above background in the PFC. Our findings suggest a need

for more commercially available radioligands for cannabinoid receptors that resolve the complications of using [3H] A-836,339 and [3H] SR141716A but confirm the utility of [3H] CP-55,940 for selectively labeling CB1 in vole tissue given the competitive assays that suggest the absence of CB2 binding in the CNS.

The presence of CB2 in neuronal tissues has been debated for decades and conclusive data have been complicated by several factors, including highly inducible receptor expression under pathological conditions, the sparsity of CB2 compared to CB1, and the issue of nonspecific antibodies (Hu & Mackie, 2015). One study provided

TABLE 4 Binding density by sex in meadow voles

Region	Females M (SEM)	Males M (SEM)	One-way ANOVA test statistics			Post hoc test statistics	
			F	df	p	d	p-Adjusted
ACA	14.6 (1.4)	14.9 (1.1)	0.017	2, 19	.898	0.057 [−0.972, 0.858]	1.000
ACB	13.7 (1.3)	13.3 (1.0)	0.067	2, 19	.799	0.113 [−0.802, 1.028]	1.000
AH	9.5 (1.5)	9.3 (1.1)	0.012	2, 19	.913	0.048 [−0.866, 0.963]	1.000
BLA	11.9 (1.2)	12.0 (0.9)	0.002	2, 19	.965	0.019 [−0.934, 0.895]	1.000
BMA	8.8 (1.0)	9.6 (0.7)	0.374	2, 19	.548	0.267 [−1.186, 0.651]	1.000
BST	10.2 (0.9)	8.8 (0.7)	1.352	2, 19	.259	0.508 [−0.421, 1.437]	1.000
CA1	20.0 (0.9)	20.5 (1.7)	0.061	2, 19	.807	0.108 [−1.023, 0.807]	1.000
CA2	18.2 (0.7)	20.8 (1.7)	1.765	2, 18	.201	0.594 [−1.554, 0.366]	1.000
CA3	18.6 (0.9)	18.6 (1.4)	.000	2, 19	1.000	.000 [−0.914, 0.915]	1.000
CEA	9.4 (0.9)	9.1 (0.8)	0.036	2, 19	.852	0.083 [−0.832, 0.998]	1.000
CP	11.8 (1.4)	10.2 (1.0)	0.936	2, 19	.345	0.423 [−0.502, 1.347]	1.000
DG	19.9 (1.8)	18.3 (1.6)	0.492	2, 19	.491	0.307 [−0.613, 1.226]	1.000
GPe	13.3 (2.2)	10.8 (1.4)	0.940	2, 19	.345	0.424 [−0.501, 1.348]	1.000
GPi	5.4 (1.0)	5.2 (0.8)	0.025	2, 19	.875	0.069 [−0.845, 0.984]	1.000
LDTh	7.4 (1.0)	6.2 (1.0)	0.791	2, 19	.385	0.389 [−0.535, 1.312]	1.000
LH	5.9 (1.1)	5.2 (0.7)	0.224	2, 18	.642	0.213 [−0.734, 1.160]	1.000
LS	13.9 (1.2)	13.0 (0.5)	0.479	2, 19	.497	0.302 [−0.617, 1.222]	1.000
MBO	8.5 (0.8)	7.8 (1.1)	0.252	2, 19	.621	0.220 [−0.698, 1.137]	1.000
MDTh	8.3 (1.0)	7.6 (1.0)	0.223	2, 19	.643	0.206 [−0.711, 1.123]	1.000
MEA	8.5 (0.9)	8.7 (0.8)	0.021	2, 19	.888	0.063 [−0.977, 0.852]	1.000
MPN	10.5 (1.1)	9.9 (0.6)	0.256	2, 19	.619	0.221 [−0.696, 1.138]	1.000
MRN	3.5 (0.8)	4.0 (0.6)	0.248	2, 18	.624	0.223 [−1.165, 0.720]	1.000
PAG	10.7 (0.9)	10.5 (1.3)	0.010	2, 19	.920	0.045 [−0.870, 0.959]	1.000
PFC	16.5 (1.3)	14.6 (1.4)	0.978	2, 19	.335	0.432 [−0.493, 1.357]	1.000
RSP	13.1 (1.3)	12.5 (1.1)	0.119	2, 19	.734	0.151 [−0.765, 1.066]	1.000
SN	25.4 (1.6)	26.3 (1.8)	0.139	2, 19	.713	0.163 [−1.079, 0.753]	1.000
SUB	17.3 (1.6)	17.2 (1.6)	0.001	2, 19	.975	0.014 [−0.901, 0.928]	1.000
VPTh	4.3 (0.9)	3.6 (0.6)	0.395	2, 18	.538	0.282 [−0.667, 1.231]	1.000
VP	9.6 (1.2)	8.0 (0.7)	1.273	2, 19	.273	0.493 [−0.435, 1.421]	1.000
VTA	7.1 (0.7)	6.7 (1.0)	0.100	2, 19	.755	0.138 [−0.777, 1.054]	1.000

Abbreviations: AH, anterior hypothalamus; ANOVA, analysis of variance; BLA, basolateral amygdala; BMA, basomedial amygdala; BST, bed nucleus of the stria terminalis; CEA, central amygdala; CP, caudate-putamen; DG, dentate gyrus; GPe, globus pallidus external; GPi, globus pallidum internal; LDTh, laterodorsal thalamus; LH, lateral hypothalamus; LS, lateral septum; MBO, mammillary bodies; MDTh, mediodorsal thalamus; MEA, medial amygdala; MOB, main olfactory bulb; MPA, medial preoptic area; MRF, reticular formation; MRN, median raphe nucleus; NAc, nucleus accumbens; PAG, periaqueductal gray; PFC, prefrontal cortex; PG, pontine gray; RSP, retrosplenial cortex; SC, superior colliculus; SN, substantia nigra; SUB, subiculum; VP, ventral pallidum; VPTh, ventroposterior thalamus; VTA, ventral tegmental area.

evidence of CB2 in the PFC of Wistar rats (Den Boon et al., 2012), but we did not find similar patterns of specific binding with our methods in voles. It is possible that the expression of CB2 varies by species within Rodentia, supporting the need for more specific anti-bodies against CB2 protein or the inclusion of more direct techniques using gene reporters as accomplished by Lopez et al. (2018) in mice. Nevertheless, however, our autoradiography results from prairie voles directly match those suggesting that CB2 may not be found in the brain of healthy rodents.

One of the most consistent features of CB1 expression is its reproducible pattern of distribution across species (Herkenham et al., 1990). Our study supports this pattern in that we did not find any evidence of regional differences in CB1 between prairie voles and meadow voles. Relative densities are also largely conserved across species; some of the regions with highest CB1 expression in rats, humans, and rhesus monkeys include the SN, CBX, and HPC (Herkenham et al., 1990). Similarly, these regions also contained high CB1 densities in the voles used for our experiment.

TABLE 5 Binding density by species

| Region	Prairie voles M (*SEM*)	Meadow voles M (*SEM*)	One-way ANOVA test statistics			Post hoc test statistics	
			F	*df*	*p*	*d*	*p*-Adjusted
ACA	16.775 (0.809)	14.739 (0.881)	2.760	2, 39	.105	0.519 [−1.162, 0.123]	.165
ACB	14.056 (1.148)	13.500 (0.804)	0.155	2, 41	.696	0.120 [−0.737, 0.497]	.696
AH	12.272 (0.873)	9.399 (0.891)	5.299	2, 41	**.026**	0.702 [−1.337, −0.067]	.070
BLA	12.983 (0.802)	11.918 (0.752)	0.916	2, 40	.344	0.295 [−0.922, 0.332]	.413
BMA	10.622 (0.611)	9.221 (0.592)	2.647	2, 40	.112	0.502 [−1.136, 0.131]	.167
BST	11.650 (0.699)	9.476 (0.574)	5.718	2, 41	**.021**	0.730 [−1.366, −0.093]	.064
CA1	23.873 (1.300)	20.269 (0.976)	4.845	2, 41	**.033**	0.672 [−1.305, −0.038]	.077
CA2	24.207 (1.138)	19.480 (0.976)	9.576	2, 40	**.004**	0.956 [−1.615, −0.297]	**.036**
CA3	22.568 (1.211)	18.614 (0.835)	7.094	2, 41	**.011**	0.813 [−1.454, −0.172]	**.047**
CEA	10.957 (0.689)	9.247 (0.578)	3.519	2, 40	.068	0.579 [−1.216, 0.058]	.113
CP	11.923 (0.880)	10.998 (0.835)	0.580	2, 41	.451	0.232 [−0.850, 0.386]	.501
DG	23.419 (1.005)	19.070 (1.152)	8.134	2, 41	**.007**	0.870 [−1.515, −0.226]	**.041**
GPe	11.223 (0.921)	11.987 (1.259)	0.243	2, 41	.625	0.150 [−0.467, 0.767]	.646
GPi	6.362 (0.506)	5.333 (0.592)	1.712	2, 40	.198	0.404 [−1.034, 0.226]	.270
LDTh	10.653 (0.726)	6.787 (0.702)	14.296	2, 40	**.001**	1.167 [−1.842, −0.492]	**.014**
LH	6.348 (0.620)	5.521 (0.621)	0.864	2, 40	.358	0.287 [−0.915, 0.340]	.413
LS	16.287 (0.992)	13.427 (0.644)	5.731	2, 41	**.021**	0.730 [−1.367, −0.094]	.064
MBO	11.079 (0.880)	8.111 (0.655)	7.216	2, 41	**.010**	0.820 [−1.461, −0.178]	**.047**
MDTh	11.490 (0.694)	7.952 (0.686)	12.822	2, 40	**.001**	1.105 [−1.775, −0.435]	**.014**
MEA	9.374 (0.568)	8.597 (0.600)	0.865	2, 40	.358	0.287 [−0.914, 0.340]	.413
MPN	12.141 (0.738)	10.207 (0.587)	4.159	2, 41	**.048**	0.622 [−1.253, 0.009]	.093
MRN	5.365 (0.511)	3.774 (0.512)	4.704	2, 40	**.036**	0.670 [−1.312, −0.028]	.077
PAG	13.387 (0.731)	10.597 (0.787)	6.759	2, 41	**.013**	0.793 [−1.433, −0.153]	**.048**
PFC	16.360 (0.983)	15.548 (0.962)	0.348	2, 41	.558	0.180 [−0.797, 0.437]	.598
RSP	15.342 (0.957)	12.779 (0.824)	4.011	2, 40	.052	0.618 [−1.257, 0.020]	.093
SN	29.060 (1.720)	25.914 (1.194)	2.217	2, 41	.144	0.454 [−1.078, 0.170]	.206
SUB	20.657 (1.020)	17.251 (1.096)	5.187	2, 41	**.028**	0.695 [−1.329, −0.060]	.070
VPTh	6.421 (0.619)	3.917 (0.531)	8.905	2, 39	**.005**	0.932 [−1.598, −0.267]	**.037**
VP	10.041 (0.856)	8.767 (0.695)	1.320	2, 41	.257	0.350 [−0.971, 0.270]	.336
VTA	8.689 (0.646)	6.917 (0.607)	3.980	2, 41	**.053**	0.609 [−1.239, 0.022]	.093

Note: Bolded numbers are *p*-values under .05.

Abbreviations: AH, anterior hypothalamus; ANOVA, analysis of variance; BLA, basolateral amygdala; BMA, basomedial amygdala; BST, bed nucleus of the stria terminalis; CEA, central amygdala; CP, caudate-putamen; DG, dentate gyrus; GPe, globus pallidus external; GPi, globus pallidum internal; LDTh, laterodorsal thalamus; LH, lateral hypothalamus; LS, lateral septum; MBO, mammillary bodies; MDTh, mediodorsal thalamus; MEA, medial amygdala; MOB, main olfactory bulb; MPA, medial preoptic area; MRF, reticular formation; MRN, median raphe nucleus; NAc, nucleus accumbens; PAG, periaqueductal gray; PFC, prefrontal cortex; PG, pontine gray; RSP, retrosplenial cortex; SC, superior colliculus; SN, substantia nigra; SUB, subiculum; VP, ventral pallidum; VPTh, ventroposterior thalamus; VTA, ventral tegmental area.

We found no evidence of sex differences in either species across any of the 45 regions we analyzed. In adult rats, the endocannabinoid system is strongly modulated by sex hormones, especially circulating levels of estradiol (López, 2010). Specifically, CB1 density and mRNA transcripts in several brain regions do fluctuate across the estrous cycle in females(de Fonseca, Cebeira, Ramos, Martín, & Fernández-Ruiz, 1994; González et al., 2000), suggesting a more dynamic role for this system in neuronal processes across the reproductive cycle in females. One study suggested that females exhibit lower CB1 densities in the hypothalamus and increased binding in the AM (Riebe, Hill, Lee, Hillard, & Gorzalka, 2010), while sex differences in hippocampal binding are more controversial (Reich, Taylor, & McCarthy, 2009; Riebe et al., 2010). Overall, relatively few papers have specifically focused on sex differences in the endocannabinoid system of any species, and those that have been published often prioritize endocannabinoid transmitters and metabolic enzymes (Craft, Marusich, & Wiley, 2013) rather than receptors. However, an important difference between rats and voles is the nature of the estrous

FIGURE 5 Comparisons of CB1 density in prairie and meadow voles. Prairie voles had higher CB1 density in CA2 and CA3 (a); DG and PAG (b); LDTh, MDTh, and VPTh (c); and in MBO (d). *p < .05. DG, dentate gyrus; LDTh, laterodorsal thalamus; MBO, mammillary bodies; MDTh, mediodorsal thalamus; PAG, periaqueductal gray; VPTh, ventroposterior thalamus [Color figure can be viewed at wileyonlinelibrary.com]
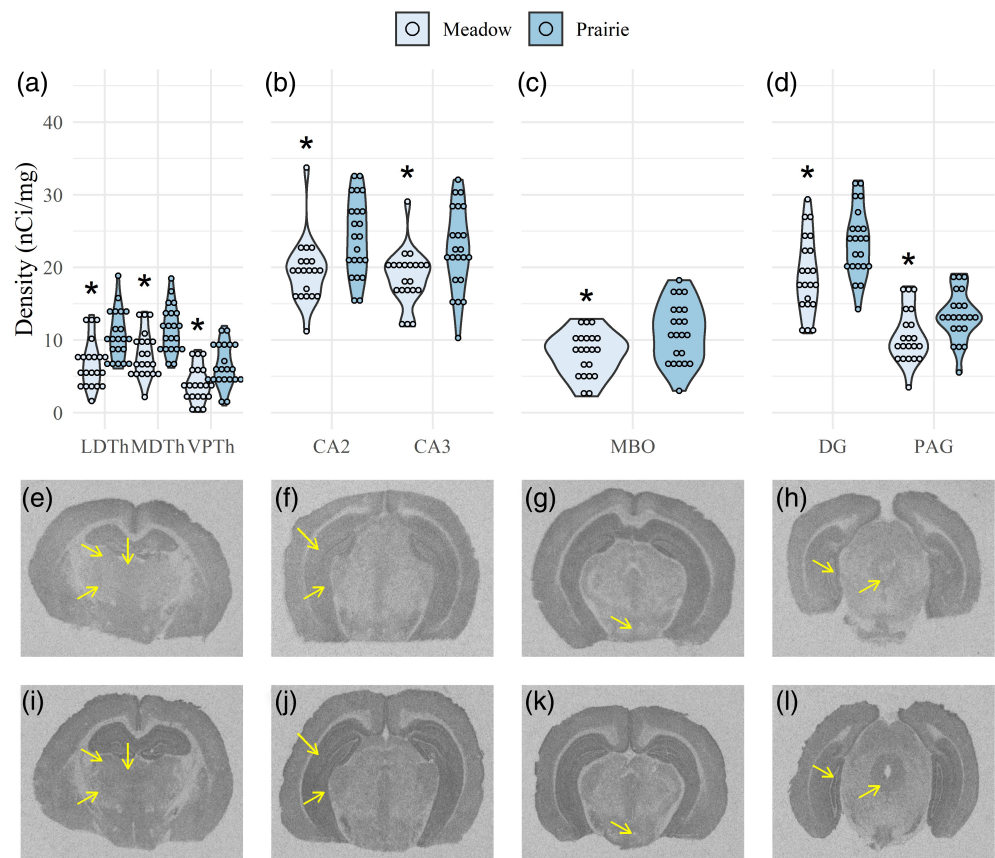
cycle. Unlike in rats, ovulation is induced in female voles by physical contact with an adult male; there is no evidence for spontaneous estrous cycles in these species (Carter et al., 1989). Since all animals used in this study were reproductively naïve, species differences in hormonal profiling may explain the lack of sex differences found in this study.

Our study revealed profound species differences in CB1 expression densities in limbic regions. Of the 30 limbic regions we analyzed, 15 of them expressed significantly different levels of CB1 across species, and in all but one of them (GPe) prairie voles had higher expression than meadow voles. With adjustments for multiple comparisons, only 8 of these 15 regions continued to show significant differences. The sheer number of regions analyzed in our study does pose a statistical problem in that most adjustments for multiple comparisons would inflate the Type II error rate. Additionally, the average effect size of the eight regions that were robust to adjustments for multiple comparisons was d = 0.932, which indicates a large effect of species on CB1 expression in these regions. However, the average effect size of the seven regions that were not robust to adjustments was still medium at d = 0.689. For this reason, it is important that this initial comparative analysis highlight all regions that were found to be statistically significant, while emphasizing those that were robust to adjustments for multiple comparisons.

CB1 densities correlate with the social organization of vole species. Specifically, the most robust differences in CB1 binding were found in regions that integrate memory with socio-spatial information.

Traditional models of the neurobiology of pair bonding emphasize regions of the brain that connect two core systems: individual recognition and the rewarding properties of mating(Aragona & Wang, 2004; Numan, 2014). However, Ophir (2017) recently suggested a third foundational component to the neurobiology of pair bonding; nonapeptides, like oxytocin and vasopressin, promote neuromodulation along memory circuits in order to evaluate the social landscape for potential mating opportunities. Critical nodes along this network included the HPC, retrosplenial cortex, LDTh, septohippocampal area, and the LS (Ophir, 2017). Many of these regions were also specifically identified in our analyses as expressing species-dependent levels of CB1, in particular the HPC, LDTh, and LS. The MBO of prairie voles also contained greater CB1 than meadow voles, and is additionally considered to be important for spatial memory (Radyushkin et al., 2005; Vann & Aggleton, 2003). As mentioned in the introduction, an intriguing link between previous comparative studies of the circuitry underlying social attachment and CB signaling is the possibility that oxytocin receptor activation may directly catalyze the production of endocannabinoids (Wei et al., 2015), at least in the ACB. Further research is warranted to explore whether the neuromodulatory effects of oxytocin (and potentially vasopressin) within socio-spatial regions of the brain are mediated through endocannabinoid mobilization.

As mentioned previously, social behaviors are likely orchestrated through a network of interconnected limbic regions called the SBNN, which includes the extended AM (e.g., BST), LS, PAG, MPN, VMH, and AH (Newman, 1999). Our study shows that monogamous prairie

voles have more CB1 than promiscuous meadow voles in these regions, aside from the VMH which was not directly measured in this study. These findings suggest that CB1 have a functionally significant role in modulating neuronal activity that contributes to the organization and expression of sociality.

In the present paper, we provide the first evidence that CB1 densities correlate with the social organization of a species, and that CB2 may not be found in healthy adult prairie voles. Specifically, monogamous voles express more CB1 in regions of the brain involved in the integration of social and spatial information. Exploring how the endocannabinoid system contributes to sociality will undoubtedly aid in our understanding of the mechanisms underlying both impact of cannabis on the social brain and in the functional interactions between various signaling systems.

CONFLICT OF INTEREST

The authors declare conflict of interest.

AUTHOR CONTRIBUTIONS

Trenton C. Simmons: Conceived, designed, acquired data, analyzed and interpreted, wrote the first draft and edited the paper. **Sara M. Freeman**: Designed, analyzed and interpreted, and edited the paper. **Nicholas S. Lackey**, **Brooke K. Dreyer**, **Devanand S. Manoli**: All contributed to acquisition and analysis of data, as well as editing of the paper; **Karen L. Bales**: Designed, analyzed and interpreted, and edited the paper.

DATA AVAILABILITY STATEMENT

The data from this manuscript are available from the authors upon reasonable request.

ORCID

Karen L. Bales https://orcid.org/0000-0001-5826-2095

REFERENCES

Albers, H. E. (2015). Species, sex and individual differences in the vasotocin/vasopressin system: Relationship to neurochemical signaling in the social behavior neural network. *Frontiers in Neuroendocrinology*, *35*, 49–71. https://doi.org/10/1016/j.yfrne.2014.07.001

Aragona, B. J., & Wang, Z. X. (2004). The prairie vole (*Microtus ochrogaster*): An animal model for behavioral neuroendocrine research on pair bonding. *ILAR Journal*, *45*(1), 35–45.

Atwood, B. K., & Mackie, K. (2010). CB2: A cannabinoid receptor with an identity crisis. *British Journal of Pharmacology*, *160*, 467–479.

Battista, N., di Tommaso, M., Bari, M., & Maccarrone, M. (2012). The endocannabinoid system: An overview. *Frontiers in Behavioral Neuroscience*, *6*(9). https://doi.org/10.3389/fnbeh.2012.00009

Boonstra, R., Xia, X., & Pavone, L. (1993). Mating system of the meadow vole, *Microtus pennsylvanicus*. *Behavioral Ecology*, *4*(1), 83–89. https://doi.org/10.1093/beheco/4.1.83

Busch, L., Sterin-Borda, L., & Borda, E. (2006). Effects of castration on cannabinoid CB1 receptor expression and on the biological actions of cannabinoid in the parotid gland. *Clinical and Experimental Pharmacology and Physiology*, *33*(3), 258–263. https://doi.org/10.1111/j.1440-1681.2006.04355.x

Carter, C. S. (1998). Neuroendocrine perspectives on social attachment and love. *Psychoneuroendocrinology*, *23*(8), 779–818 Retrieved from http://www.ncbi.nlm.nih.gov/pubmed/9924738

Carter, C. S., DeVries, A. C., & Getz, L. L. (1995). Physiological substrates of mammalian monogamy: The prairie vole model. *Neuroscience and Biobehavioral Reviews*, *19*(2), 303–314 Retrieved from http://www.ncbi.nlm.nih.gov/pubmed/7630584

Carter, C. S., Witt, D. M., Manock, S. R., Adams, K. A., Bahr, J. M., & Carlstead, K. (1989). Hormonal correlates of sexual behavior and ovulation in male-induced and postpartum estrus in female prairie voles. *Physiology & Behavior*, *46*(6), 941–948 Retrieved from http://www.ncbi.nlm.nih.gov/pubmed/2699360

Castelli, M. P., Fadda, P., Casu, A., Spano, M. S., Casti, A., Fratta, W., & Fattore, L. (2014). Male and female rats differ in brain cannabinoid CB1 receptor density and function and in behavioural traits predisposing to drug addiction: Effect of ovarian hormones. *Current Pharmaceutical Design*, *20*(13), 2100–2113. https://doi.org/10.2174/13816128113199990430

Craft, R. M., Marusich, J. A., & Wiley, J. L. (2013). Sex differences in cannabinoid pharmacology: A reflection of differences in the endocannabinoid system? *Life Sciences*, *92*(8–9), 476–481. https://doi.org/10.1016/j.lfs.2012.06.009

de Fonseca, F. R., Cebeira, M., Ramos, J. A., Martín, M., & Fernández-Ruiz, J. J. (1994). Cannabinoid receptors in rat brain areas: Sexual differences, fluctuations during estrous cycle and changes after gonadectomy and sex steroid replacement. *Life Sciences*, *54*(3), 159–170. https://doi.org/10.1016/0024-3205(94)00585-0

den Boon, F. S., Chameau, P., Schaafsma-Zhao, Q., van Aken, W., Bari, M., Oddi, S., … Werkmana, T. R. (2012). Excitability of prefrontal cortical pyramidal neurons is modulated by activation of intracellular type-2 cannabinoid receptors. *Proceedings of the National Academy of Sciences of the United States of America*, *109*(9), 3534–3539. https://doi.org/10.1073/pnas.1118167109

DeVries, M. S., Cordes, M. A., Rodriguez, J. D., Stevenson, S. A., & Riters, L. V. (2016). Neural endocannabinoid CB1 receptor expression, social status, and behavior in male European starlings. *Brain Research*, *1644*, 240–248. https://doi.org/10.1016/j.brainres.2016.05.031

Egertová, M., & Elphick, M. R. (2000). Localisation of cannabinoid receptors in the rat brain using antibodies to the intracellular C-terminal tail of CB1. *Journal of Comparative Neurology*, *422*(2), 159–171. https://doi.org/10.1002/(SICI)1096-9861(20000626)422:2<159::AID-CNE1>3.0.CO;2-1

Freundt-Revilla, J., Kegler, K., Baumgärtner, W., & Tipold, A. (2017). Spatial distribution of cannabinoid receptor type 1 (CB1) in normal canine central and peripheral nervous system. *PLoS One*, *12*(7), 1–21. https://doi.org/10.1371/journal.pone.0181064

Getz, L. L., Carter, C. S., & Gavish, L. (1981). The mating system of the prairie vole *Microtus ochrogaster*: Field and laboratory evidence for pair-bonding. *Behavioral Ecology and Sociobiology*, *8*, 189–194.

González, S., Bisogno, T., Wenger, T., Manzanares, J., Milone, A., Berrendero, F., … Fernández-Ruiz, J. J. (2000). Sex steroid influence on cannabinoid CB1 receptor mRNA and endocannabinoid levels in the anterior pituitary gland. *Biochemical and Biophysical Research Communications*, *270*(1), 260–266. https://doi.org/10.1006/bbrc.2000.2406

Grinevich, V., & Neumann, I. D. (2020). Brain oxytocin: How puzzle stones from animal studies translate into psychiatry. *Molecular Psychiatry*, *8*, 1–15. https://doi.org/10.1038/s41380-020-0802-9

Gruder-Adams, S., & Getz, L. L. (1985). Comparison of the mating system and paternal behavior in *Microtus ochrogaster* and *M. pennsylvanicus*. *Journal of Mammalogy*, 66(1), 165–167.

Herkenham, M., Lynn, A. B., Little, M. D., Johnson, M. R., Melvin, L. S., de Costa, B. R., & Rice, K. C. (1990). Cannabinoid receptor localization in brain. *Proceedings of the National Academy of Sciences of the United States of America*, 87(5), 1932–1936 Retrieved from http://www.pnas.org/content/87/5/1932.abstract

Herkenham, M., Lynn, A. B., de Costa, B. R., & Richfield, E. K. (1991). Neuronal localization of cannabinoid receptors in the basal ganglia of the rat. *Brain Research*, 547(2), 267–274. https://doi.org/10.1016/0006-8993(91)90970-7

Hu, S. S.-J., & Mackie, K. (2015). Distribution of the endocannabinoid system in the central nervous system. In R. G. Pertwee (Ed.), *Endocannabinoids. Handbook of Experimental Pharmacology*, 231, 59–93. Cham: Springer. https://doi.org/10.1007/978-3-319-20825-1_3

Insel, T. R., & Shapiro, L. E. (1992). Oxytocin receptor distribution reflects social organization in monogamous and polygamous voles. *Proceedings of the National Academy of Sciences of the United States of America*, 89 (13), 5981–5985.

Jansen, E. M., Haycock, D. A., Ward, S. J., & Seybold, V. S. (1992). Distribution of cannabinoid receptors in rat brain determined with aminoalkylindoles. *Brain Research*, 575(1), 93–102. https://doi.org/10.1016/0006-8993(92)90428-C

Lopez, A., Aparicio, N., Pazos, M. R., Grande, M. T., Barreda-Manso, M. A., Benito-Cuesta, I., ... Romero, J. (2018). Cannabinoid CB2 receptors in the mouse brain: Relevance for Alzheimer's disease. *Journal of Neuroinflammation*, 15, 158. https://doi.org/10.1186/s12974-018-1174-9

López, H. H. (2010). Cannabinoid-hormone interactions in the regulation of motivational processes. *Hormones and Behavior*, 58(1), 100–110. https://doi.org/10.1016/j.yhbeh.2009.10.005

Matsuda, L. A., Lolait, S. J., Brownstein, M. J., Young, A. C., & Bonner, T. I. (1990). Structure of a cannabinoid receptor and functional expression of the cloned DNA. *Nature*, 346, 561–564. https://doi.org/10.1038/346561a0

Matsuda, L. A., Bonner, T. I., & Lolait, S. J. (1993). Localization of cannabinoid receptor mRNA in rat brain. *Journal of Comparative Neurology*, 327(4), 535–550. https://doi.org/10.1002/cne.903270406

Munro, S., Thomas, K. L., & Abu-Shaar, M. (1993). Molecular characterization of a peripheral receptor for cannabinoids. *Nature*, 365, 61–65.

Newman, S. W. (1999). The medial extended amygdala in male reproductive behavior: A node in the mammalian social behavior network. *Annals of the New York Academy of Sciences*, 877, 242–257.

Numan, M. (2014). *Neurobiology of social behavior: Toward an understanding of the prosocial and antisocial brain*. Waltham, MA: Elsevier Science Publishers.

Ophir, A. G. (2017). Navigating monogamy: Nonapeptide sensitivity in a memory neural circuit may shape social behavior and mating decisions. *Frontiers in Neuroscience*, 11(JUL), 397. https://doi.org/10.3389/fnins.2017.00397

Pamplona, F. A., & Takahashi, R. N. (2012). Psychopharmacology of the endocannabinoids: Far beyond anandamide. *Journal of Psychopharmacology*, 26(1), 7–22. https://doi.org/10.1177/0269881111405357

Pertwee, R. G. (2000) Cannabinoid receptor ligands: clinical and neuropharmacological considerations, relevant to future drug discovery and development. *Expert Opin Investig Drugs 9*, 1553-1571. https://doi.org/10.1517/13543784.9.7.1553

Pertwee, R. (2010). Receptors and channels targeted by synthetic cannabinoid receptor agonists and antagonists. *Current Medicinal Chemistry*, 17(14), 1360–1381. https://doi.org/10.2174/092986710790980050

R Core Team. (2019). *R: A language and environment for statistical computing*, Vienna, Austria: R Foundation. Retrieved from https://www.r-project.org

Radyushkin, K., Anokhin, K., Meyer, B. I., Jiang, Q., Alvarez-Bolado, G., & Gruss, P. (2005). Genetic ablation of the mammillary bodies in the Foxb1 mutant mouse leads to selective deficit of spatial working memory. *European Journal of Neuroscience*, 21(1), 219–229. https://doi.org/10.1111/j.1460-9568.2004.03844.x

Ramikie, T. S., Nyilas, R., Bluett, R. J., Gamble-George, J. C., Hartley, N. D., Mackie, K., ... Patel, S. (2014). Multiple mechanistically distinct modes of endocannabinoid mobilization at central amygdala glutamatergic synapses. *Neuron*, 81(5), 1111–1125. https://doi.org/10.1016/j.neuron.2014.01.012

Reich, C. G., Taylor, M. E., & McCarthy, M. M. (2009). Differential effects of chronic unpredictable stress on hippocampal CB1 receptors in male and female rats. *Behavioural Brain Research*, 203(2), 264–269. https://doi.org/10.1016/j.bbr.2009.05.013

Riebe, C. J. N., Hill, M. N., Lee, T. T. Y., Hillard, C. J., & Gorzalka, B. B. (2010). Estrogenic regulation of limbic cannabinoid receptor binding. *Psychoneuroendocrinology*, 35, 1265–1269. https://doi.org/10.1016/j.psyneuen.2010.02.008

Roberts, R. L., Miller, A. K., Taymans, S. E., & Carter, C. S. (1998). Role of social and endocrine factors in alloparental behavior of prairie voles (*Microtus ochrogaster*). *Canadian Journal of Zoology*, 76(10), 1862–1868.

Roberts, R. L., Williams, J. R., Wang, A. K., & Carter, C. S. (1998). Cooperative breeding and monogamy in prairie voles: Influence of the sire and geographical variation. *Animal Behaviour*, 55, 1131–1140.

Shapiro, L. E., & Insel, T. R. (1992). Oxytocin receptor distribution reflects social organization in monogamous and polygynous voles. *Annals of the New York Academy of Sciences*, 652, 448–451.

Tamarin, R. H. (1985). *Biology of New World Microtus*, Stillwater, OK: American Society of Mammalogists.

Torchiano, M. (2018). *effsize: Efficient effect size comparison*. Zenodo Retrieved from https://doi.org/10.5281/zenodo.1480624

van Sickle, M. D., Duncan, M., Kingsley, P. J., Mouihate, A., Urbani, P., Mackie, K., ... Sharkey, K. A. (2005). Identification and functional characterization of brainstem cannabinoid CB2 receptors. *Science*, 310 (5746), 329–332. https://doi.org/10.1126/science.1115740

Vann, S. D., & Aggleton, J. P. (2003). Evidence of a spatial encoding deficit in rats with lesions of the mammillary bodies or mammillothalamic tract. *Journal of Neuroscience*, 23(8), 3506–3514. https://doi.org/10.1523/jneurosci.23-08-03506.2003

Wei, D., Lee, D., Cox, C. D., Karsten, C. A., Peñagarikano, O., Geschwind, D. H., ... Piomelli, D. (2015). Endocannabinoid signaling mediates oxytocin-driven social reward. *Proceedings of the National Academy of Sciences of the United States of America*, 112(45), 14084–14089.

Yoshida, T., Uchigashima, M., Yamasaki, M., Katona, I., Yamazaki, M., Sakimura, K., ... Watanabe, M. (2011). Unique inhibitory synapse with particularly rich endocannabinoid signaling machinery on pyramidal neurons in basal amygdaloid nucleus. *Proceedings of the National Academy of Sciences of the United States of America*, 108(7), 3059–3064. https://doi.org/10.1073/pnas.1012875108